ADAPTIVE TURBO-EQUALIZER DESIGN FOR MULTI-USER MOBILE COMMUNICATION CHANNEL

A. Kundu, B. K. Sarkar, and A. Chakrabarty

Kalpana Chawla Space Technology Cell (KCSTC)
Department of Electronics & Electrical Communication Engineering
Indian Institute of Technology
Kharagpur-721 302, West Bengal, India

Abstract—Broadband single carrier modulated signals experience severe multipath distortion scrambling & ISI when propagating through physical medium. Correcting the distortion with channel equalization is the foremost task of the detector. Prior information about the transmitted signals in the form of channel decoder feedback can significantly enhance equalization accuracy. An algorithm that iteratively performs channel decoding and equalization with prior information is generally denoted turbo-equalizer. Turbo-Equalizer uses prior information & the principle of interference cancellation by MMSE criterion. Here we have tested Adaptive Turbo Equalization with least Mean Square Algorithm (LMS) & modified normalized LMS algorithm & Turbo-Decoding with a Log-Map. Consequently the Mean Square Error analysis, Stability analysis and convergence analysis are provided and its shown if the system is sparse, then the system will converge faster for a given total asymptotic MSE, though the choice of initialization is important. Here all the Implementation concepts have been verified in MATLAB platform and evaluation of the proposal is presented. The measurement for the performance is displayed as bit error rates (BER) in comparison to SNR of the Channel.

1. INTRODUCTION

This work focuses on Turbo coding & decoding, modulation & demodulation, channel model with ISI, turbo equalization, sparsity analysis of the proposed system. Adaptive Turbo Equalizer consists of two basic parts i.e., decision feedback equalizer and maximum-a-posteriori MAP decoder [5–8]. In a mobile communication environment there are several users and each channel is associated with error control

coding with turbo codes, modulation with QAM & spreading by CDMA. All the users signal are added on to the channel. Simplified model is shown in the Fig. 1. A usual assumption for wireless transmission channels is that AWGN occurs. Also ISI can be noticed originating from multiple paths scattering and delaying the signal. At the receiver , one of the best method for getting the information back from , often heavily scrambled & distorted received signal is to use turbo scheme [6–8], it can significantly improve the process of eliminating interference.
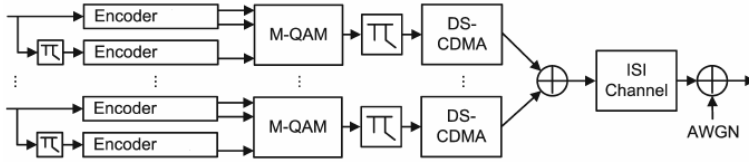

Figure 1. Turbo transmitter with ISI & AWGN in the channel.

The system shown in the Fig. 1 consists of a transmitter that uses a turbo code of the length K. the information data block denoted by x_n for N users parallel, where vector x stands for a discrete time sequence; $x_n = x_n[K] = \{x_n[0], x_n[1], \ldots, x_n[K-1]\}$ for users $n = 1, 2, 3, \ldots, N$ and $k = 0, 2, \ldots, K-1$. All the successions of $\log_2(M)$ bits of these encoded sequences $x_{TC,n}$ are mapped to a QAM modulation constellation of order M and interleaved each user QAM symbol sequences. $x_{QAM,n}$ is spread by multiplication with a user specific spreading sequence having DSCDMA coding, resulting in a block of spread data symbol denoted by $x_{CDMA,n}$. These are then simultaneously transmitted through the channel as a summed up signal x_{CDMA}. This channel experiences ISI & AWGN with different levels of selectivity. At the receiver end an adaptive channel estimator uses a training sequence to find the optimum tap coefficients for the equalizer. The usual RAKE receiver [11–13] would not yield sufficient performance due to interference. The signal r is thus processed by an adaptive equalizer, consisting of LMS or NLMS algorithm [25] & leads to estimation of $\hat{x}_{CDMA}$. Next a matched filter adjusted to users spreading sequences & estimates [12–15] the modulation symbols of this user $\hat{x}_{QAM,1}$. Simultaneously one user is selected in the Log-map among the user of interest. This technique is called Multi-User Detection (MUD) [4–7]. The common term takes into account that it has to be regained from the multiuser signal and all users' data could be detected parally in the same manner. After de-interleaving & demodulation the sequence $\hat{x}_{TC,1}$ has to be decoded by the Turbo

decoder [6–9], producing the estimation of this user's data $\hat{x}_1$ and extrinsic information about bit probability for iterative use of the whole Turbo scheme Receiver. Fig. 1 shows Turbo scheme transmitter, source producing independent, identically distributed data sequence x_n of length K for all N users. Data blocks are encoded by a Turbo coder. For simulation we have used two binary convolutional coder having code rate $R_{BCE} = \frac{n_{BCE}}{k_{BCE}} = 1/2$.

Here n_{BCE} & k_{BCE} are no of in and output of the convolutional coder respectively. Here two recursive systematic convolutional (RSC) codes with generator polynomial $g1 = 23_{oct}$ & $g2 = 37_{oct}$ are used. The generator polynomial notation is in octal corresponding binary values are $g1 = 10011$ & $g2 = 11111$. In delay tap it can be shown as $g1 = D + D^3 + D^4$ & $g2 = D + D^1 + D^2 + D^3 + D^4$. A convolutional encoder produces an output that is $(k + v)/R_{BCE}$ bits longer than the input due to general action of the coder to add redundancy of rate R_{BCE} and the additional tail of $\frac{v}{R_{BCE}}$ bits. These come from the last encoder back to an all zero state. This results a problem of 'fractional rate loss', a drop of the code rate (Real $< R_{BCE}$) can be handled by either tail biting or truncation. One of the two Binary Convolutional Codes (BCEs') is fed directly with the data sequence x_n. The other one with an interleaved version of it Д (x_n). Д is the symbol for an interleaver, which defines a permutation of all bits, providing uncorrelated possible errors for the receiver Ⅱ indicates the sign of de-interleaver.

2. M-ARY QAM MODULATION

Modulation is a mapping of binary data to a continuous time & valued signal. It presents an effective way of increasing the BW of a data transmission system. The basic idea is to map the input data to a constellation in the complex plane, thus using in phase & quadrature components i.e., employing in phase & quadrature carriers [12–14]. The RF transmit signal for use would be given by;

$$S_n(t) = R\left\{\left(\sum_{k=-\infty}^{\infty} x_{QAM,n}[k]g(t - kT)\right) e^{j2*pi*f_c*t}\right\} \qquad (1)$$

with

$$R\{x_{QAM,n}[k]\}, I\{x_{QAM,n}[k]\} \in \left\{-\sqrt{M}+1, \ldots, -1, -1, 1, 3, \ldots \sqrt{M}-1\right\} \qquad (2)$$

where $R[.]$ and $I[.]$ denote real & imaginary part & $g(t)$ is the signal pulse. $x_{QAM,n}[k] = A_{I,n}[k] + jA_{Q,n}[k]$ will be used where $A_{I,n}[k]$

& $A_{Q,n}[k]$ are the amplitude levels calculated from the $\log_2(M)/2$ bits each of the in phase & quadrature component. From practical experience it has been seen that higher modulation order results in dense constellation, as the altogether available power is assumed to be restricted and the symbol position have to move closer together. The energy per symbol E_s increase with $\log_2(M)$ while the number of constellation point increases with M. when average energy per bit $E_b = \dfrac{\sum_k |x_{QAM,n}[k]|^2}{K*\log_2(M)} = 1$ is normalized to 1, the distance between neighboring points decreases with increasing M. The dense structures are more vulnerable to noise as slighter distortions can already push a symbol to a neighboring symbols detection region. Yet the usable constellation depends on the channel, its SNR and other disturbances [19–22].

3. THE CHANNEL MODEL

For the model of a wireless mobile communication channel [15–18] to be realistic, it has to include many aspects, fading phase & frequency distortion, inter-symbol, co-channel & multiple access interference, near far cross talk as well as colored and white noise also influences a transmitter [19, 21, 24]. Here we will model only AWGN & ISI referred in Fig. 2. The functional channel equation is $r = Hx_{CDMA} + w$. Where H is the ISI channel can be seen as a delay spread in time or as multipath fading [17–19, 22, 26] and can be modeled by a tapped delay line.
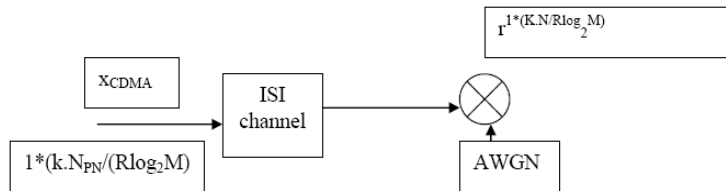

Figure 2. Fundamental channel model with AWGN & ISI.

Its consequences is that the Nyquist criterion is isolated and each symbol is blurred by surrounding symbols which can leads to erasement and total loss of reliable information as decision threshold cannot be reconstructed by modeling the channel, this problem can be overcome with equalization. In addition to the interference also AWGN is a common problem in wireless communication channels.

This is produced as Gaussian distributed thermal noise in electronic device. And SNR is defined as $SNR = 10\log_{10}(\frac{E_b}{N_0})$, where $N_0/2$ corresponds to two sided power spectral density. This explains SNR allows a comparison of performances with respect to the transmitted bits not symbols. Fig. 3 refers to the magnitude & frequency response characteristics of the Microwave channel under investigation.
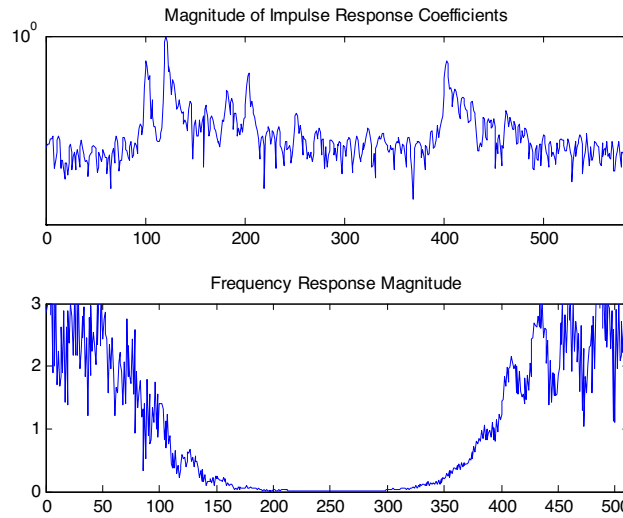

Figure 3. Magnitude & frequency response of the microwave channel under investigation.
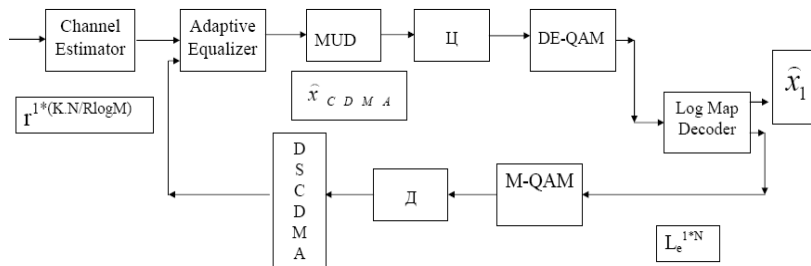
4. TURBO-SCHEME RECEIVER

Figure 4. Turbo receiver block-diagram.

The receiver [1–3] has to reverse all the modifications, processing steps and influences that were done to the user's data in inverse order. That implies it has to overcome the noise and interference of the physical transmission by channel estimation and equalization to detect single users out of the multi user babble, to de-interleave and demodulate and finally to decode the Turbo Code (TC).
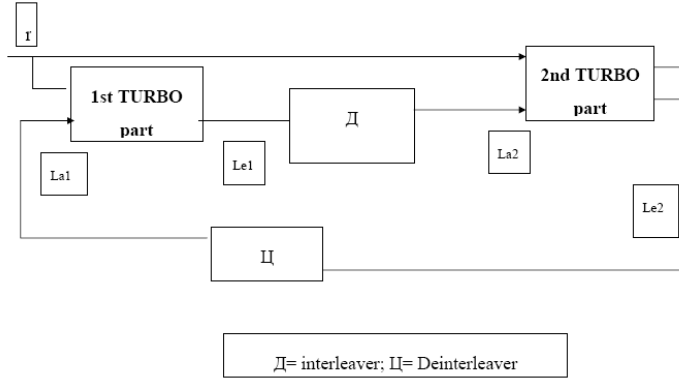

Figure 5. Information flow in a turbo-decoding scheme.

As each of the steps on the transmission side added some kind of coding gain to increase the reliability of the transmission, all the parts of the receiver help to enhance the performance in regard to achievable bit error rate. This is done iteratively in a turbo manner i.e., with the help of side information about bit probabilities gained. The information flow in a general turbo decoding scheme can be shown in the Fig. 5. The received sequence serves as input to both decoder parts, but each uses only part of sequences that was generated by one of the encoder. The extrinsic information (L_{e1}, L_{e2}) gained by soft decisions from one decoder part is used as a priori side information (L_{a2}, L_{a1}) for the other and vice versa. It is important however, that no information gained from one decoder, as the positive feedback would mean an unstable system. The log-like hood ratio (LLR) for bit probabilities have two main advantages, first lower computational complexity and secondly a direct & demonstrative measure for the probability as well as sign of each bit. The extrinsic information is calculated by the following formula $L_{e,a} = LLR = \log \frac{f_{x'}(x'_k = +1|_{r_k})}{f_{x'}(x'_k = -1|_{r_k})}$ where x'_k and r_k as an exception more generally denote the estimated and the input signal of the according decoder stage respectively. The objective of channel estimation can be divided into two distinctive

parts, the primary channel estimation by sending a training sequence and the subsequent improvement of this estimation in the equalizer. So instead of generating a special training sequence at the transmitter and sending it in front of the actual data after all the encoding steps, the MATLAB implementation simply generates a single user random BPSK sequence of length K_{tr} and applies the same channel model (ISI & AWGN) to it, as only the influence of the channel is of interest for channel estimation. So first the channel estimator tries to equalize the distortion during training by assuming the sequence to be known at the receiver & then to obtain the optimum filter parameters, and then the data is equalized accordingly to this (several times iteratively repeated) first estimation. The special adaptive turbo equalization improves this channel estimation by "tracking" in a decision directed mode during Turbo equalization process, i.e., not only from one data symbol, the filter tap coefficients is updated (referred in Fig. 6), but also from one iteration to the next. The advantage is that the system learns to adapt the environment.
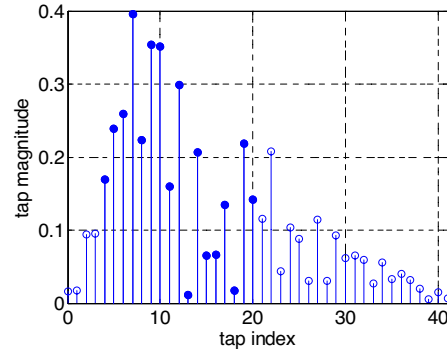

Figure 6. The tap magnitude & indexing in a particular instant of learning.

The main part of this estimation is an adaptive decision feedback equalizer as shown in the Fig. 7. The feed forward & feedback filter of such a DFE are FIR filters with L_f & L_b symbol spaced taps having adjustable coefficients f_l & b_l. As there is a recursive structure from the detector output to the feedback filter, it has nonlinear characteristics. Its soft output will be in the mathematical form as

$$\widehat{x}_{CDMA}[K] = \sum_{l=1}^{L_f} f_l r[k-l] - \sum_{l=1}^{L_b} b_l \widehat{x}_{fb}[k-l], \text{ where } \widehat{x}_{fb} = sign(\widehat{x}_{CDMA})$$
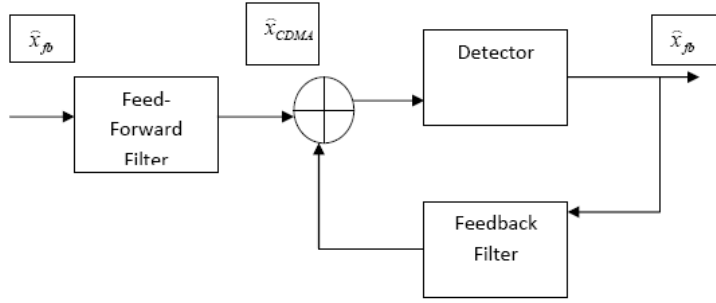
$$(3)$$

Figure 7. Adaptive decision feedback equalizer with feed forward filter.

This is used in first iteration, from the second iteration on the feedback filter coefficients b_l are approximated and calculated from the priori information so that $\widehat{x}_{fb} = 2a$. The advantage we find here over a linear equalization or a zero forcing equalizer, primarily its capability to handle ISI channels with spectral nulls, but DFE [7–10] are not the optimum equalizer solutions in terms of performances. It is obvious that the simulated result of MMSE MAP sequence detectors performances is better than having higher computational complexity. We may use any adaptive update algorithm, for simplicity here we took MMSE, LMS, and Sharp LMS, NLMS for the mathematical simulation.

$$f[k] = f[k-1] + \mu_f e[k] r[k]; \quad b[k] = b[k-1] - \mu_b e[k] \widehat{x}_{fb}[k]$$

where μ_f & μ_b are the adaptation constants i.e., step sizes for adaptation and $e[k] = L_a[k] - \widehat{x}_{CDMA}[k]$; at each time instant k LMS algorithm tries to minimize the MSE by estimating the gradient vector of the method of steepest descent. By the choice of the step size the speed of the convergence can be influenced. Larger step size bring a faster convergence but we need to compromise for higher fluctuation of the minimum error noise floor. The selection of good step size is a very good critical task even though we find some theoretical limits like $0 < \mu < \frac{1}{t_r(R)}$; where $t_r(R)$ denotes the trace of the input autocorrelation matrix for adaptive Turbo Equalizer usually only much smaller yields the desired convergence effect. In digital implementation the computational precision limits the lower end of useful adaptation coefficients. An optimum μ_{opt} is hence always a compromise and can be in practice minimizing the cost function. Beside the famous Widrow's LMS method there are several more modified adaptive algorithms. According to the published literature NLMS algorithm [25] can be

expressed as

$$W[k] = W[k-1] + \mu_w e[k] F_q(X[k]) \tag{4}$$

Here

$$[F_q(X[k])]_l = \frac{|x_l[k]|^{q-1} \, sign(x_l[k])}{\displaystyle\sum_{m=1}^{L} |x_m[k]|^q} \quad \text{if} \quad 1 \le q < \infty$$

or

$$\frac{1}{x_n[k]} \delta_{i-n} \quad \text{if} \quad q = \infty$$

where $W[k]$ represents the filter taps, $X_1[k]$ is the L_{fb} samples of the input signals in the filter memory at time k, δ_j is the kronecker delta function & n is any integer for which $|x_n[k]| = \max_{1 < j \le L} |x_j[k]|$. The minimization of $\|W[k+1] - W[k]\|$ with respect to $x[k] - W_{k+1}^T X_k = 0$ shows the optimization problem. The filter coefficient adaptation is explained by

$$W_l[k+1] = w_l[k] + \mu_w e[k] x_i[k] \quad \text{if} \quad |x_i[k]| = \max_{1 < j < L} |x_j[k]|$$

$$\text{otherwise} \quad w_l[k]$$

Here w_l stands for f_l or b_l respectively and x denotes either r or $\widehat{x}_{fb}$. The error calculated as $x[k] - \widehat{x}_{CDMA}^T[k] b_k$ only one filter coefficients is updated at each time for $q = \infty$, the algorithm yields a version of NLMS that minimizes L_∞-norm, simple but better performance, is called modified NLMS [25]. Its cost function has very small optimum region.

5. SHARPNESS ANALYSIS OF PROPOSED ALGORITHM FOR TURBO-EQUALIZATION

The sequence $\widehat{y}_k$ is assumed to be generated from input data x_k in a linear way following the equation $\widehat{y}_k = \sum_i w_k^i x_k^i$.

The weight vector $w_k = [w_k^1, \ldots, w_k^n]$ is updated at each iteration k by $x_k w_{k+1}^i = w_k^i + \mu w_k^i (y_k - \widehat{y}_k) x_k^i$ where μ is a small step size. The general update strategy may be approximated

$$w_{k+1}^i = w_k^i \exp\left(\mu \frac{\delta L(y_k, \widehat{y}_k)}{\delta w_k^i}\right) \tag{5}$$

where cost function is $L(y_k, \widehat{y}_k) = (y_k - \widehat{y}_k)^2$. This approximation involves taking a Taylor series expansion of the exponential dropping

term of μ^2 or higher. The last expression can be modified by estimating y_k by $w_k^i = \gamma(z_k^i) = \frac{1}{4}(z_k^i)^2$ for some parameter value z. now if we take the algorithm as adapting over z space we can use Euclidean gradient descent

$$Z_{k+1}^i = z_k^i - \mu \frac{\delta L(y_k, \widehat{y}_k)}{\delta z_k^i} \tag{6}$$

The gradient term becomes

$$\frac{\delta L}{\delta(\widehat{y}_k)} \cdot \frac{\delta(\widehat{y}_k)}{\delta w_k^i} \cdot \frac{\delta(w_k^i)}{\delta z_k^i} = -2(y_k - \widehat{y}_k)x_k^i \gamma(z_k^i) \tag{7}$$

Now we absorb the factor 2 into step size to get $Z_{k+1}^i = z_k^i + \mu\gamma(z_k^i)(y_k - \widehat{y}_k)x_k^i$. Here we are truly interested in the effective update rule for w, not z and that is used to generate our estimate y_k; since $w_{k+1}^i = \gamma(z_{k+1}^i) = \gamma(z_k^i + \text{Small term})$, in most of signal processing & communication application the weights are not constrained to be positive, as is required by this update rule. So for simplicity here we take

$$\widehat{y}_k = \sum_i sgn(z_k^i)(z_k^i)^2 x_k^i \tag{8}$$

and Euclidean gradient algorithm in z space becomes

$$Z_{k+1}^i = z_k^i + \mu \left| z_k^i \right| (y_k - \widehat{y}_k)x_k^i \tag{9}$$

and effective update for z space will be

$$w_{k+1}^i = w_k^i + \mu \left(2 \left| w_k^i \right| + t^2 \right) \left(y_k - \widehat{y}_k \right) x_k^i \tag{10}$$

In order to gain some insight as to the shape of the cost surface in z space such that the algorithm referred here evolves over the intuition gained from a 10 tap filter under design. Here the equation referred has been compared with standard widrow's LMS algorithm and named as sharp LMS algorithm and parameterized as

$$w_k^i = \gamma \left(z_k^i \right) = \frac{1}{2} sgn \left(z_k^i \right) \left(z_k^i \right)^2 + \varepsilon x_k^i; \tag{11}$$

so the vector z, that get mapped by γ onto w. for readers consequences this is to say that both are gradient descent algorithm & the Fig. 8 refers the plot of cost surface over which they are evolving. Fig. 8 shows the standard LMS with MSE cost $L = E(y_k - \widehat{y}_k)^2$ over which LMS evolves, as LMS is gradient descent in w space, so the axes are the parameter w_1 & w_2. In contrast sharp LMS is a gradient descent

of the same cost function but gradient is with respect to z so Fig. 9 referred is the MSE cost plotted against axes z_1 & z_2. Fig. 10 & Fig. 11 refer the Change of MSE with symbol number and change of the tap value with number of taps.
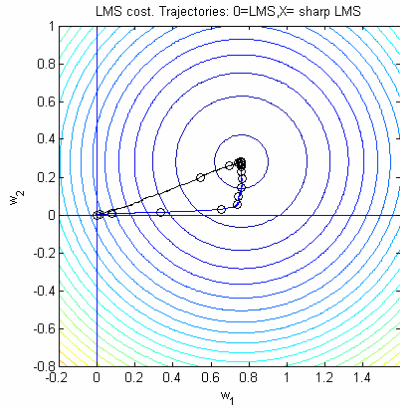

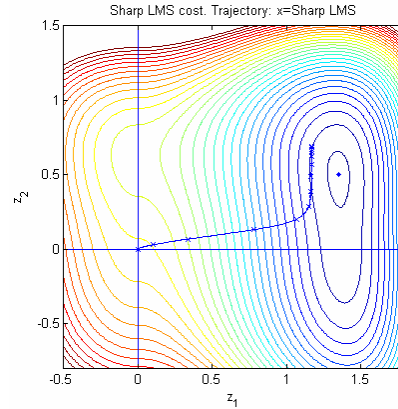**Figure 8.** Standard LMS with MSE cost surface.
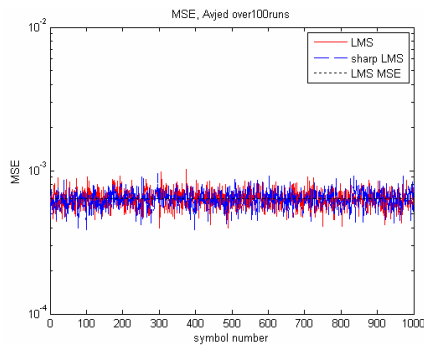

Figure 9. Sharp LMS with MSE cost surface.

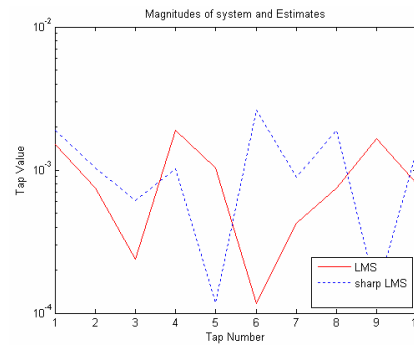**Figure 10.** Symbol number with MSE plot for Turbo Equalizer following Descent algorithm.

Figure 11. Change of tap value with tap number.

6. LOG-MAP TURBO DECODER

The second Turbo part in the Fig. 5 is the decoder for Turbo Code (TC). After the decoding the information can be restored at least with higher like hood ratios, allowing a more exact estimation of the coded sequence. The additional knowledge can then later be used again in

the next iteration for equalization and so on. The TURBO CODE itself again consists of two of the iteratively connected parts dealing with two consistent codes. The main principle is to use LLR with expression

$$L(x[k]) = \log \frac{p(x[k] = +1|_r)}{p(x[k] = -1|_r)} \tag{12}$$

The Turbo trellis diagram description changes this equation to a complicated one

$$L(x[k]) = \log \frac{\frac{\sum_{s^+} P(S[k-1] = s', s[k] = s, r)}{P(r)}}{\frac{\sum_{s^-} P(S[k-1] = s', s[k] = s, r)}{P(r)}} = \log \frac{\sum_{s+} P(s', s, r)}{\sum_{s-} P(s', s, r)}; \tag{13}$$

here $s^{\pm}$ are the sets of all trellis state transmitting from a state s' to s caused by a data input of ± 1. Hence the input sequence is denoted as the received signal r as this is the usual case for Turbo coding. The previous equation can be reduced as $P(s', s, r) = \alpha_{k-1}(s') \cdot \gamma_k(s', s) \cdot \beta_k(s)$ with the necessary probabilities $\alpha_{k-1}(s') = P(s[k] = s, r_1^k)$, $\gamma_k(s', s) = P(s[k] = s, r[k] | s[k-1] = s'$ and $\beta_k(s) = P(r_{k+1}^N | s[k] = s)$.

Using the advantage of iterative decoding repetitions, the equation can be rearranged in the following fashion

$$L(x_k) = \log \frac{P(r | x_k = +1)}{P(r | x_k = -1)} + \log \frac{P(x_k = +1)}{P(x_k = -1)}; \tag{14}$$

This second term of this equation stands for a priori LLR that would be 0 in a conventional decoding scheme without this kind of side information about certain bit probabilities.

Figure 14 explains that this Log-Map decoder is actually used iteratively to decode two turbo parts. But when the equalizer is used as a decoder for ISI channel as first of the two turbo parts this would lead to a iterative loop within a loop. Use of extrinsic LLR information $\widehat{x}_1$ about coded bit probabilities gained from decoding as a priori information L_a in the equalizer has to be rearranged comparable to the directly received signal. Therefore like on the transmission side, it has to run through modulation, interleaving and CDMA spreading to be in correct order. Fig. 12 refers the error history of adaptation with NLMS algorithm. It is obvious from the figure that error is converging and convergence time is such that the real-time implementation possible. Fig. 13 shows channel frequency response normalized to baud frequency.
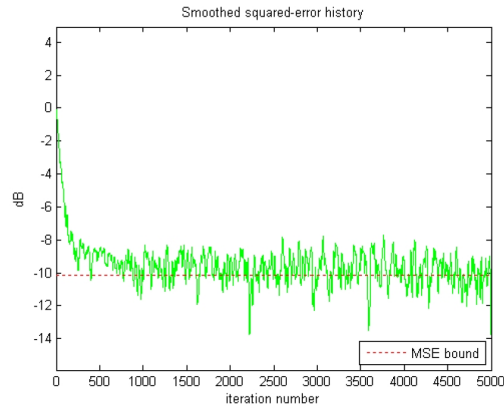
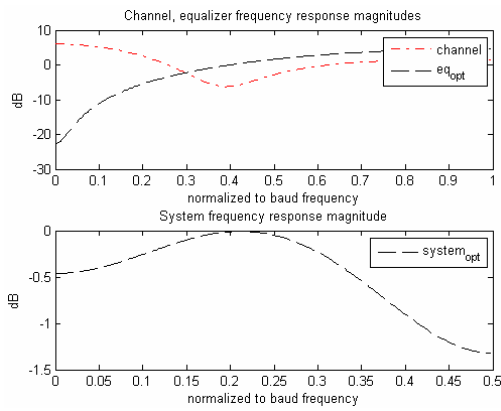**Figure 12.** Equalizer error history with iteration number; number of tap:6 with NLMS algo.

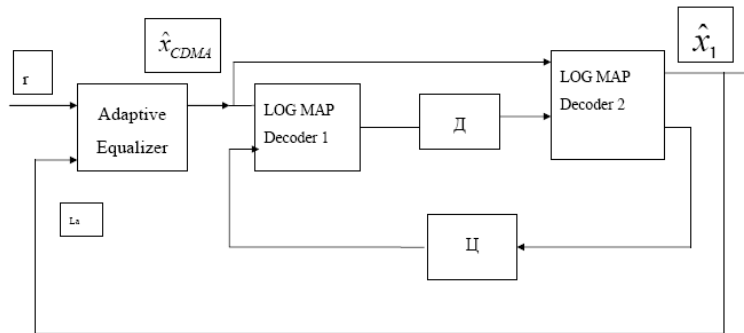**Figure 13.** Channel frequency response normalized to baud frequency.

Figure 14. Turbo receiver block with LOG-MAP decoder.

Figure 15 shows the channel & combined channel equalizer after implementing the turbo coding. Fig. 16 shows cost & achievable bit rate versus the iteration number. The fact the cost is not monotonically decreasing in the first few hundreds samples, its because of the initial stage the algorithm no longer be a perfect gradient descent algorithm (though it in approximately so). From Fig. 17, it can be said that adaptive turbo equalizer can rapidly provide a solution approximately the Max SNR solution. Fig. 18 shows BER curves for system employing (using various adaptive algorithm) turbo equalization and without turbo equalization. The data point for each SNR values was obtained by averaging over all carriers for the block & repeating for a total of two channel realization.
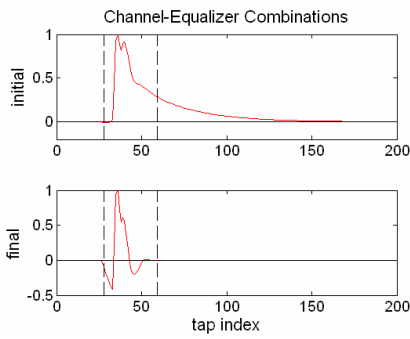

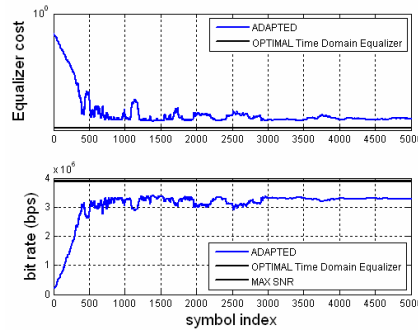**Figure 15.** Initial and final tap index for Turbo Equalizer.

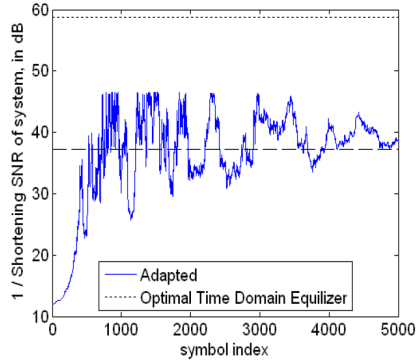**Figure 16.** Achievable bit-rate versus time.

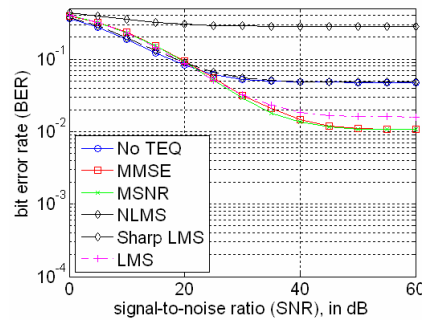**Figure 17.** Inverse of shortened SNR versus time.

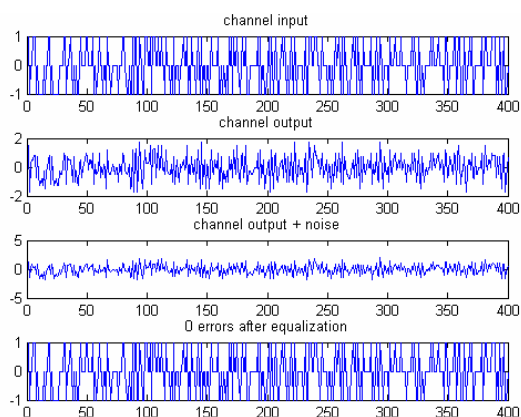**Figure 18.** BER vs SNR for the wireless channel under Test.

Figure 19. Channel input output introduces noise and zero errors after channel equalization.

7. CONCLUSION

Equalization of multiple user mobile channels is implemented observed and evaluated which requires exhaustive mathematical calculations. All the simulations have been done in MATLAB version 7.14. Turbo Equalizer with various form of steepest descent algorithm shows after equalization we can extract the exact bit patterns with zero errors (referred in Fig. 19). The results suggest that the procedure is well suited for multicarrier system with global convergence of algorithm.

ACKNOWLEDGMENT

REFERENCES

1. Lee, F. K. H. and P. J. Mclane, "Parallel-trellis turbo equalizers for sparse-coded transmission over SISO and MIMO sparse multipath channels," *IEEE Transactions on Wireless Communications*, Vol. 5, Issue 12, 3568–3578, December 2006.
2. Jordan, F. and K.-D. Kammeyer, "On the application of turbo equalizers in GSM compatible receivers," *URSI International*

Symposium on Signals, Systems, and Electronics, 1998. ISSSE 98, 460–464, Sept. 29–Oct. 2, 1998.

3. Peacock, M. J. M. and I. B. Collings, "Mutual information analysis of turbo equalizers for fixed and fading channels," *IEEE International Conference on Communications, 2003. ICC '03*, Vol. 4, 2938–2942, May 11–15, 2003.

4. Trajkovic, V. and P. Rapajic, "Adaptive decision feedback turbo equalization and multiuser detection," *2004 IEEE Eighth International Symposium on Spread Spectrum Techniques and Applications*, 540–544, Aug. 30–Sept. 2, 2004.

5. Vogelbruch, F., R. Zukunft, and S. Haar, "16-QAM turbo equalization based on minimum mean squared error linear equalization," *Conference Record of the Thirty-Sixth Asilomar Conference on Signals, Systems and Computers, 2002*, Vol. 2, 1943–1947, Nov. 3–6, 2002.

6. Liu, Z., J. Wang, C. Zhao, J. Wang, and M. Jiang, "A novel turbo equalization for MIMO frequency selective fading channels," *2006 International Conference on Communications, Circuits and Systems Proceedings*, Vol. 2, 1063–1067, June 25–28, 2006.

7. Park, J. and S. B. Gelfand, "Sparse MAP equalizers for turbo equalizations," *IEEE 61st Vehicular Technology Conference, 2005*, Vol. 2, 762–766, May 30–June 1, 2005.

8. Song, S., A. C. Singer, and K.-M. Sung, "Turbo equalization with an unknown channel," *IEEE International Conference on Acoustics, Speech, and Signal Processing, 2002. Proceedings. (ICASSP '02)*, Vol. 3, III-2805–III-2808, May 13–17, 2002.

9. Kim, J.-H. and Y.-H. You, "Pilot-free frequency tracking method for ultra-wideband receivers," *Progress In Electromagnetics Research*, PIER 82, 65–75, 2008.

10. Lee, Y.-D., D.-H. Park, and H.-K. Song, "Improved channel estimation and MAI-robust schemes for wireless of DMA system," *Progress In Electromagnetics Research*, PIER 81, 213–223, 2008.

11. Mishra, M. and S. Konar, "High bit rate dense dispersion managed optical communication systems with distributed amplification," *Progress In Electromagnetics Research*, PIER 78, 301–320, 2008.

12. Tripathi, R., R. Gangwar, and N. Singh, "Reduction of crosstalk in wavelength division multiplexed fiber optic communication systems," *Progress In Electromagnetics Research*, PIER 77, 367–378, 2007.

13. Kamitsos, I. and N. K. Uzunoglu, "Improvement of transmission properties of multimode fibers using spread spectrum technique

and a rake receiver approach," *Progress In Electromagnetics Research*, PIER 76, 413–425, 2007.

14. Tarhuni, N. G., M. Elmusrati, and T. Korhonenn, "Multi-Class Optical-CDMA network using optical power control," *Progress In Electromagnetics Research*, PIER 64, 279–292, 2006.

15. Kundu, A. and A. Chakrabarty, "Fractionally spaced constant modulus algorithm for wireless channel equalization," *Progress In Electromagnetics Research B*, Vol. 4, 237–248, 2008.

16. Usman, M., R. A. Abd-Alhameed, and P. S. Excell, "Design considerations of MIMO antennas for mobile phones," *PIERS Online*, Vol. 4, No. 1, 121–125, 2008.

17. Wang, W., Y. Zhang, K. Zhou, and H. Zhang, "Research on asymmetric characteristics of mobile communications system based on electromagnetic radiation," *PIERS Online*, Vol. 3, No. 8, 1298–1302, 2007.

18. Arnetz, B. B., T. Akerstedt, L. Hillert, A. Lowden, N. Kuster, and C. Wiholm, "The effects of 884 MHz GSM wireless communication signals on self-reported symptom and sleep (EEG) — An experimental provocation study," *PIERS Online*, Vol. 3, No. 7, 1148–1150, 2007.

19. Wang, F., Y. Xiong, and X. Yang, "Approximate ML detection based on MMSE for MIMO systems," *PIERS Online*, Vol. 3, No. 4, 475–480, 2007.

20. Zhao, J., J. Zhou, N. Xie, J. Zhai, and L. Zhang, "Error analysis and compensation algorithm for digital predistortion systems," *PIERS Online*, Vol. 2, No. 6, 702–705, 2006.

21. Abouda, A. A., H. M. El-Sallabi, L. Vuokko, and S. G. Häggman, "Spatial smoothing effect on kronecker MIMO channel model in urban microcells," *Journal of Electromagnetic Waves and Applications*, Vol. 21, No. 5, 681–696, Apr. 2007.

22. Li, H.-J., T.-Y. Liu, and J.-L. Leou, "Antenna measurements in the presence of multipath waves," *Progress In Electromagnetics Research*, PIER 30, 157–178, 2001.

23. Ohta, M., Y. Mitani, and H. Ogawa, "Multi-dimensional generalization in space and time domains for Middleton's study in stochastic evaluation of correlative many EM noise processes," *Progress In Electromagnetics Research*, PIER 24, 97–118, 1999.

24. Wang, X., P. R. P. Hoole, and E. Gunawan, "An electromagnetic-time delay method for determining the positions and velocities of mobile stations in a GSM network," *Progress In Electromagnetics Research*, PIER 23, 165–186, 1999.

25. Kundu, A. and A. Chakrabarty, "Frequency domain NLMS algorithm for enhanced jam resistant GPS receiver," *Progress In Electromagnetics Research Letters*, Vol. 3, 69–78, 2008.

26. Khani, H. and P. Azmi, "Performance analysis of a high data rate UWB-DTR system in dense multipath channels," *Progress In Electromagnetics Research B*, Vol. 5, 119–131, 2008.